ISSN: 2664-9640

Kinematic Analysis and Path Planning of a Delta Parallel Manipulator for the Selective Harvesting of Premium Tea

Wei Tang, Changlin Song*, Qin Huang, Junmin Li, Jun Bai

School of Mechanical Engineering, Xihua University, Chengdu 610039, Sichuan, China

*Corresponding author: Changlin Song

Abstract

The fine harvesting of premium tea is currently performed by hand and is therefore labour-intensive and inefficient. This paper presents a harvesting scheme based on a Delta parallel manipulator and investigates the kinematic behaviour and the harvesting path-planning problem of the mechanism. A kinematic model of the Delta manipulator is established, the forward and inverse position solutions and the velocity Jacobian matrix are derived, and the workspace and the distribution of singular configurations are analysed. On the basis of the spatial distribution of buds and leaves in the tea canopy, a spatial distribution model of the harvesting target points is established and the matching between the manipulator workspace and the harvesting region is evaluated. A hierarchical path-planning method is then proposed for the premium-tea harvesting scenario: the harvesting target points are partitioned into sub-regions by density clustering, a traversal path is solved within each sub-region by an improved ant colony algorithm, and the trajectory is smoothed and optimised subject to the kinematic constraints of the Delta manipulator. Simulation results show that, compared with conventional traversal planning, the proposed method shortens the total path length by 14.8 %, reduces the total harvesting time by 18.8 % and the maximum jerk of the trajectory by 34.1 %, and improves the computational efficiency by 72.1 %, and that it adapts better to the unstructured premium-tea harvesting scenario.

Keywords

Delta Manipulator; Kinematic Analysis; Premium Tea Harvesting; Spatial Distribution; Path Planning; Trajectory Optimisation.

1. Introduction

1.1. Background and Significance

As a high-value product of the tea industry, premium tea is subject to strict quality requirements regarding the integrity of the plucked shoot, its freshness and the morphology of the bud and leaf. At present, premium tea is produced mainly by manual selective plucking of “one bud and one leaf” or “one bud and two leaves”. This operation is labour-intensive, inefficient and costly, and because the labour demand is concentrated in the tea season, the industry has long suffered from a seasonal labour shortage, which severely restricts the scaling-up and standardisation of premium-tea production [1]. As population ageing intensifies and rural labour continues to migrate to other sectors, the shortcomings of manual plucking have become more pronounced. Promoting the mechanisation and intelligent upgrading of premium-tea harvesting has therefore become an inevitable trend for removing this bottleneck and improving the economic return of tea production.

Tea-plucking machinery as a whole is evolving from rough cut-and-collect operation towards refined selective intelligent plucking. Early conventional tea-plucking machines were based on cutting, harvesting the surface layer of the canopy by reciprocating or spiral cutting. Although

ISSN: 2664-9640

the productivity per pass is high, such machines cannot identify or grade the buds and leaves, the harvested material is mixed and the product quality is poor, so they cannot meet the plucking standard for premium tea at all. In recent years, with the rapid development of machine vision, robot control and intelligent planning, selective plucking robots with precise recognition and point-specific plucking capability have become a research focus in tea machinery, offering a new technical route towards damage-free and efficient mechanised harvesting of premium tea. Against this background, this paper takes a Delta parallel manipulator as the actuator and studies the key technologies of intelligent premium-tea harvesting. Because the workspace of the manipulator is considerably smaller than the harvesting region of a tea canopy, the matching between the two is treated here as a design problem in its own right rather than as an assumption, and it is quantified in Section 3.3. The work is of theoretical value and engineering significance for the domestic manufacture of high-end tea-harvesting equipment and for improving the quality and efficiency of the premium-tea industry.

1.2. State of the Art

1.2.1. Harvesting Machinery and Actuators

In the development of tea-harvesting machinery, a clear pattern of technological iteration has emerged in China and abroad. Research abroad started earlier and the technology is more mature: Abhiram et al. reviewed the four generations of tea-harvesting machinery, identified computer-vision-based intelligent selective plucking machines as the core future direction of the industry, and pointed out that intelligent tea-plucking equipment generally struggles to reconcile plucking accuracy with operating efficiency. The development of Chinese tea-harvesting machinery has followed essentially the same path, relying initially on cutting-type machines for bulk tea and, in recent years, focusing on intelligent selective plucking technology and equipment for the fine harvesting of premium tea [2].

With regard to the selection and application of harvesting actuators, serial manipulators and Cartesian manipulators are the mainstream conventional solutions for tea-plucking robots in China and abroad. Chinese researchers have designed a four-degree-of-freedom gantry tea-plucking robot based on a DSP controller, whose three-axis coordinated operation reaches 2517 operations per hour, and have adopted a SCARA manipulator as the plucking actuator together with a neural-network adaptive compensation controller that effectively improves trajectory tracking accuracy. A large body of work nevertheless shows that, under the high-speed and light-load conditions of tea plucking, serial manipulators generally suffer from insufficient structural stiffness, rapid degradation of end-effector accuracy at high speed and poor stability, and are therefore ill-suited to the fine, low-damage plucking required for premium tea. Compared with serial mechanisms, the Delta parallel manipulator offers high stiffness, high speed and high accuracy, and has been widely applied in light-load high-speed tasks such as food packaging and electronic sorting. Its structural characteristics match the requirements of tea plucking closely, which makes it a preferred actuator for premium-tea plucking robots.

1.2.2. Kinematic Analysis and Path Planning of Manipulators

In the field of Delta manipulator kinematics, a fairly complete theoretical foundation has been established. Researchers abroad have carried out systematic work on mechanism modelling, workspace analysis and singularity identification: a physical model of the Delta robot workspace was established and performance atlases were drawn to support dimensional optimisation; kinematic analysis of the mechanism was completed and a MATLAB simulation GUI was developed; and the kinematics and singular configurations of a four-degree-of-freedom Delta mechanism were analysed and several singularity criteria were compared. In addition, closed-loop kinematic chains were systematically classified with respect to singular

ISSN: 2664-9640

configurations and the concept of constraint singularity was proposed, which completed the singularity theory of lower-mobility parallel mechanisms [3]. Chinese studies are mostly engineering adaptations of the above theories, focusing on improving the operational stability of the manipulator by simulation modelling; customised parameter matching and spatial adaptation for the particular working conditions of tea-garden harvesting are, however, rarely addressed.

With regard to path and trajectory planning, existing work can be divided into trajectory optimisation of industrial manipulators and multi-target harvesting path planning in agriculture. For the industrial pick-and-place operation of a Delta manipulator, the operating cycle has been optimised on the basis of a Pythagorean-hodograph curve, a quintic B-spline curve has been used to achieve high-order trajectory smoothing, and an improved quintic B-spline planning method has been proposed in combination with dynamic stress characteristics, effectively improving the efficiency and smoothness of the manipulator in industrial scenarios [4]. In agricultural harvesting, researchers have formulated multi-target harvesting sequence planning for fruit and vegetable picking as a travelling salesman problem (TSP) or a multiple travelling salesman problem (MTSP) and have optimised the harvesting path by intelligent algorithms such as clustering, genetic algorithms and ant colony algorithms, effectively improving the efficiency of multi-target picking.

Overall, existing research provides solid theoretical and technical support for the application of the Delta manipulator to tea plucking, but clear gaps remain for premium-tea harvesting. The buds and leaves of the tea plant are randomly and densely distributed over the canopy in an unstructured manner, which differs markedly from fixed industrial target points and from sparse fruit and vegetable picking scenarios, and conventional planning algorithms are computationally inefficient and adapt poorly to kinematic constraints. Yang et al. proposed a hybrid trajectory optimisation strategy for premium-tea harvesting that is optimal in time and jerk, but did not fully consider the influence of the spatial distribution of buds and leaves on the harvesting path [5]. Research on spatial matching modelling of the manipulator and on hierarchical intelligent path planning for densely and randomly distributed target points in the premium-tea harvesting scenario therefore remains limited, and this is the entry point of the present study.

2. Kinematic Analysis of the Delta Harvesting Manipulator

2.1. Mechanism Description and Coordinate Systems

The Delta parallel manipulator consists of a fixed platform, a moving platform and three identical limbs. Schematic diagram of the structure of the Delta manipulator is shown in Figure 1. Each limb comprises a drive arm and a driven arm; the drive arm is actuated by a motor mounted on the fixed platform, and the driven arm is a parallelogram linkage connected to the end of the drive arm and to the moving platform by spherical joints. The parallelogram linkage constrains the orientation of the moving platform, so that it remains horizontal throughout the motion and possesses only three translational degrees of freedom. This structural design gives the Delta manipulator high stiffness, high speed and high accuracy, which matches the requirements of light-load high-speed harvesting closely [6].

ISSN: 2664-9640

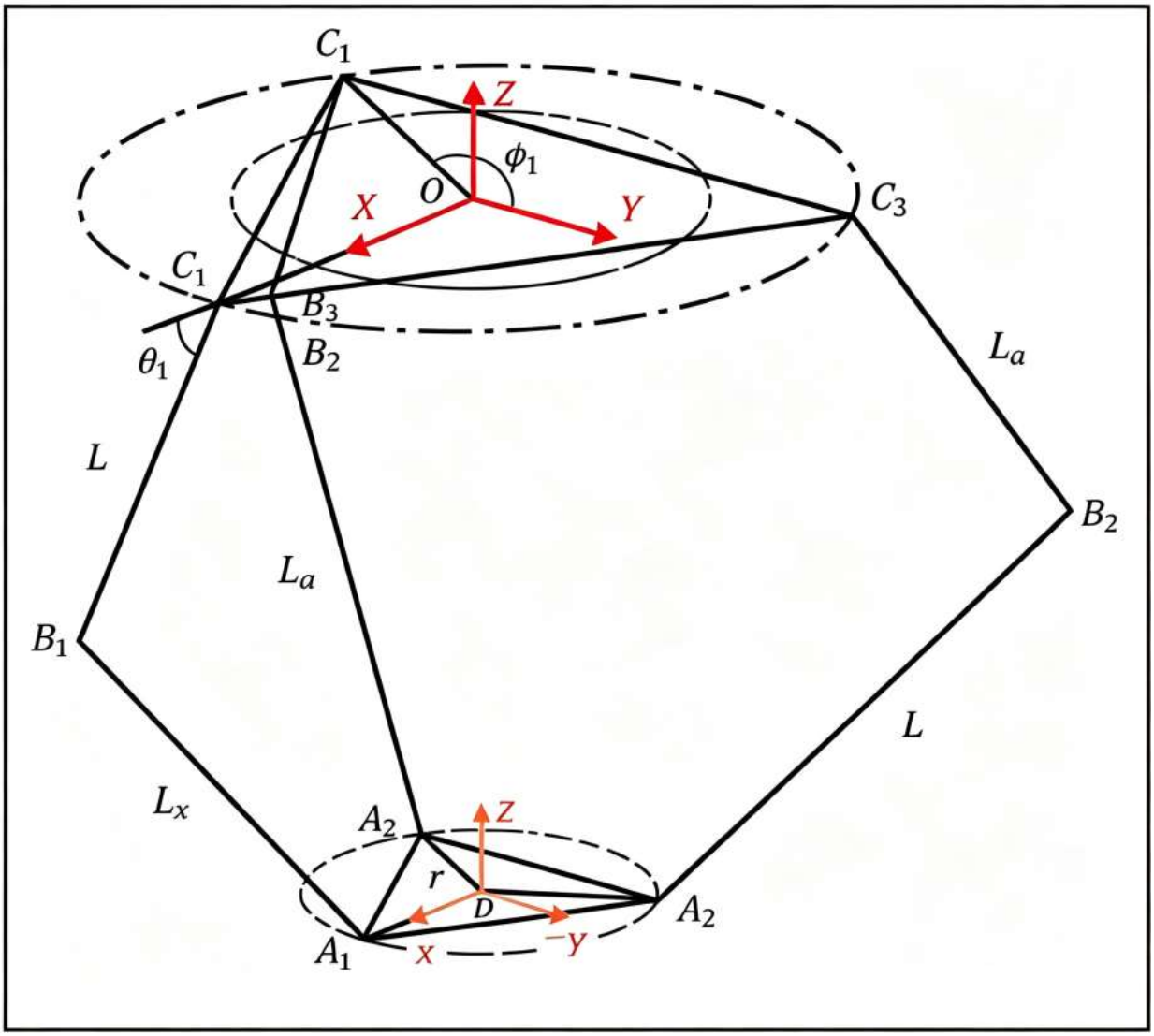


Figure 1. Schematic diagram of the structure of the Delta manipulator.

To establish the kinematic model, the following coordinate systems are defined. The fixed frame O-XYZ is attached to the centre of the fixed platform with its origin O at that centre, the Z axis pointing vertically upwards and the X axis pointing towards the hinge centre of the first drive arm. The moving frame o-xyz is attached to the centre of the moving platform with its origin o at that centre, and its axes are parallel to those of the fixed frame.

The structural parameters are defined as follows: R is the radius of the circle on which the centres of the three drive hinges on the fixed platform lie, r is the radius of the circle on which the centres of the three driven hinges on the moving platform lie, L is the length of the drive arm and l is the length of the driven arm. The drive angles of the three drive arms are denoted θ_1, θ_2 and θ_3; rotation downwards from the horizontal plane of the upper surface of the fixed platform is taken as positive.

2.2. Position Analysis

2.2.1. Inverse Position Solution

The inverse position solution determines the three drive angles from the known position $P = (x, y, z)$ of the centre of the moving platform, that is it solves for $\theta_i (i = 1,2,3)$.

ISSN: 2664-9640

Let the centre of the drive hinge of limb i on the fixed platform be A_i and the centre of the driven hinge on the moving platform be B_i. By symmetry, the three points A_i are evenly distributed on the fixed platform, with coordinates

$$A_i = (R\cos\alpha_i, R\sin\alpha_i, 0), \quad i = 1,2,3 \tag{1}$$

where $\alpha_i = 2\pi(i-1)/3$ is the azimuth angle of the i-th limb.
Similarly, the coordinates of the three points B_i on the moving platform are

$$B_i = (x + r\cos\alpha_i, y + r\sin\alpha_i, z), \quad i = 1,2,3 \tag{2}$$

The coordinates of the end point C_i of the drive arm are

$$C_i = (R\cos\alpha_i + L\cos\theta_i\cos\alpha_i, R\sin\alpha_i + L\cos\theta_i\sin\alpha_i, -L\sin\theta_i) \tag{3}$$

Since the length of the driven arm is the constant l, the distance between C_i and B_i is identically equal to l:

$$\|B_i - C_i\|^2 = l^2 \tag{4}$$

Substituting the coordinates of B_i and C_i into the above expression and rearranging yields a quadratic equation in θ_i:

$$E_i\cos\theta_i + F_i\sin\theta_i = G_i \tag{5}$$

in which the coefficients E_i, F_i and G_i are determined by the structural parameters and the position of the moving platform. Using trigonometric identities, the solution is obtained as

$$\theta_i = 2\arctan\left(\frac{F_i \pm \sqrt{E_i^2 + F_i^2 - G_i^2}}{E_i + G_i}\right) \tag{6}$$

where the positive and negative signs correspond to the two assembly modes. For the conventional Delta robot configuration, the solution in which the moving platform lies below the drive arms is usually selected, that is the positive sign is taken.

2.2.2. Forward Position Solution

The forward position solution determines the position θ_i of the centre of the moving platform from the three known drive angles $P = (x, y, z)$. The forward position solution of a Delta parallel robot is comparatively complex and generally requires the solution of a set of nonlinear equations. In this paper a numerical iterative method is used, taking the result of the inverse position solution as the initial value and approaching the true solution progressively by Newton-Raphson iteration [7].

Let the drive angle vector be $\boldsymbol{\theta} = [\theta_1, \theta_2, \theta_3]^T$ and the end-effector position vector be $\boldsymbol{p} = [x, y, z]^T$. The forward problem can then be stated as finding $\boldsymbol{\theta}$ from the known $\boldsymbol{p}$, subject to the constraint equations

ISSN: 2664-9640

$$f_i(\boldsymbol{p}, \theta_i) = \|B_i - C_i\|^2 - l^2 = 0, \quad i = 1,2,3 \tag{7}$$

Given the end-effector position $\boldsymbol{p}_0$ corresponding to the initial drive angles, the solution is corrected iteratively according to

$$\boldsymbol{p}_{k+1} = \boldsymbol{p}_k - \mathbf{J}_f^{-1}(\boldsymbol{p}_k)\boldsymbol{f}(\boldsymbol{p}_k) \tag{8}$$

where $\mathbf{J}_f$ is the Jacobian matrix of the constraint equations with respect to the end-effector position. When the iteration error falls below a prescribed threshold the iteration converges and the end-effector position is obtained.

2.3. Velocity Analysis and the Jacobian Matrix

Velocity analysis establishes the mapping between the drive joint velocities and the velocity of the moving platform. Differentiating both sides of the inverse position solution with respect to time gives

$$\mathbf{J}_x\dot{\boldsymbol{p}} = \mathbf{J}_\theta\dot{\boldsymbol{\theta}} \tag{9}$$

where $\dot{\boldsymbol{p}} = [\dot{x}, \dot{y}, \dot{z}]^T$ is the velocity vector of the moving platform and $\dot{\boldsymbol{\theta}} = [\dot{\theta}_1, \dot{\theta}_2, \dot{\theta}_3]^T$ is the vector of drive joint velocities. $\mathbf{J}_x$ and $\mathbf{J}_\theta$ are the Jacobian sub-matrices associated with the end-effector velocity and the joint velocity, respectively.

Rearranging gives

$$\dot{\boldsymbol{\theta}} = \mathbf{J}\dot{\boldsymbol{p}} \tag{10}$$

where $\mathbf{J} = \mathbf{J}_\theta^{-1}\mathbf{J}_x$ is the inverse Jacobian matrix of the Delta manipulator.

The forward velocity mapping follows as

$$\dot{\boldsymbol{p}} = \mathbf{J}^{-1}\dot{\boldsymbol{\theta}} \tag{11}$$

The Jacobian matrix not only expresses the velocity mapping but is also an important tool for analysing the singularity, dexterity and force transmission characteristics of the manipulator [8].

2.4. Workspace and Singular Configurations

2.4.1. Workspace Determination

The workspace of the Delta manipulator is the set of all spatial points that the centre of the moving platform can reach. Three-dimensional view of the workspace for Delta manipulator is shown in Figure 2. In this paper the workspace is determined numerically: within a prescribed spatial range all candidate points are traversed with a fixed step size and the inverse position solution is evaluated at each point; if a solution exists and satisfies the joint angle limits, the point belongs to the workspace.

The joint angle constraints are

$$\theta_{\min} \le \theta_i \le \theta_{\max}, \quad i = 1,2,3 \tag{12}$$

ISSN: 2664-9640

where θ_{min} and θ_{max} are the lower and upper limits of the drive angle, respectively.

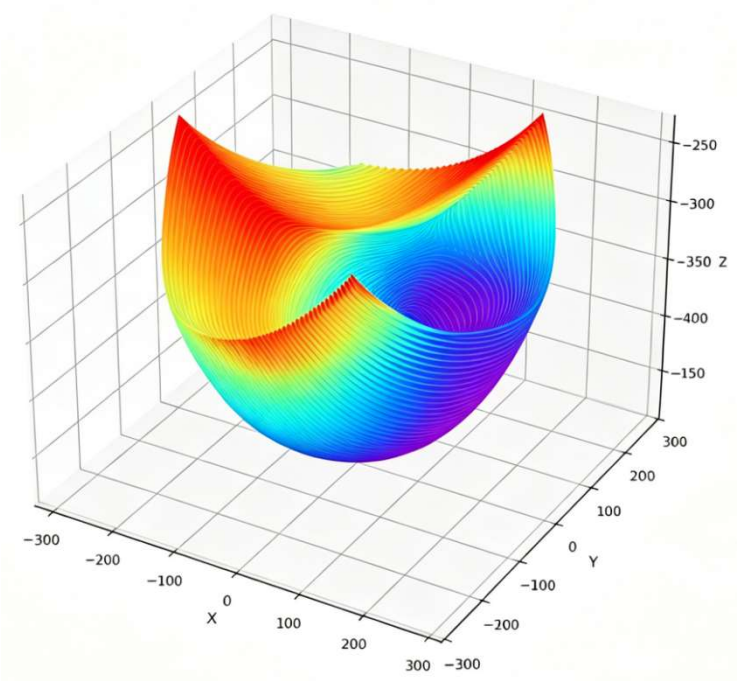


Figure 2. Three-dimensional view of the workspace for Delta manipulator

2.4.2. Singular Configurations

A singular configuration of a parallel manipulator is a configuration in which the Jacobian matrix loses rank; the manipulator then loses or gains certain degrees of freedom, which leads to failure of motion control or abnormal force transmission. According to the classification of Gosselin and Angeles, three types of singular configuration exist for parallel robots [9]:

An inverse singularity occurs when $\mathbf{J}_\theta$ is singular. The drive joints can then no longer impose force or torque constraints on the moving platform and the manipulator loses its ability to resist external forces. For the Delta manipulator, inverse singularities usually occur at the boundary of the workspace.

A forward singularity occurs when $\mathbf{J}_x$ is singular. Even with the drive joints locked, the moving platform may still undergo a small motion, so the number of degrees of freedom of the manipulator increases. As a three-degree-of-freedom purely translational parallel mechanism, the Delta manipulator generally has no forward singularity inside its normal workspace.

A combined singularity occurs when $\mathbf{J}_x$ and $\mathbf{J}_\theta$ are singular simultaneously; the input and output of the manipulator are then completely decoupled.

In this paper the dexterity distribution of the manipulator within the workspace is evaluated by computing the condition number of the Jacobian matrix. The smaller the condition number, the better the isotropy of the manipulator and the more uniform the motion transmission:

$$\kappa = \|\mathbf{J}\| \cdot \|\mathbf{J}^{-1}\| \tag{13}$$

When the condition number tends to infinity the manipulator is in a singular configuration. In path planning, regions in which the condition number is excessively large should be avoided as far as possible in order to guarantee smooth and controllable motion.

ISSN: 2664-9640

3. Spatial Distribution of the Premium-tea Harvesting Targets

3.1. Canopy Morphology and the Distribution of Buds and Leaves

The objects of premium-tea harvesting are the tender shoots on the surface of the tea canopy, mainly “one bud and one leaf” and “one bud and two leaves”. The morphology of the canopy and the distribution of the buds and leaves directly affect the working mode and the path-planning strategy of the harvesting robot.

After pruning and harvesting management, the canopy of a tea plant usually presents an arched or flat plucking table. Schematic diagram of the spatial distribution of buds and leaves in the tea canopy is shown in Figure 3. The canopy width is generally between 1.0 m and 1.5 m and the canopy height is about 0.8 m to 1.2 m. The buds and leaves are distributed mainly within 0 cm to 15 cm below the canopy surface, in a three-dimensional arrangement. In the horizontal direction the distribution is uneven: influenced by illumination, branch density and pruning practice, there are pronounced differences in density.

From the point of view of spatial distribution, the buds and leaves in the tea canopy have the following characteristics. First, the distribution region is large: the harvesting area covered by a single tea plant may reach several square metres. Second, the number of target points is large: in the peak season tens to hundreds of harvestable buds and leaves may be distributed over each square metre of canopy. Third, the spatial distribution is random and clustered: buds and leaves tend to grow in clusters along the direction of branch growth, forming a number of dense regions [10].

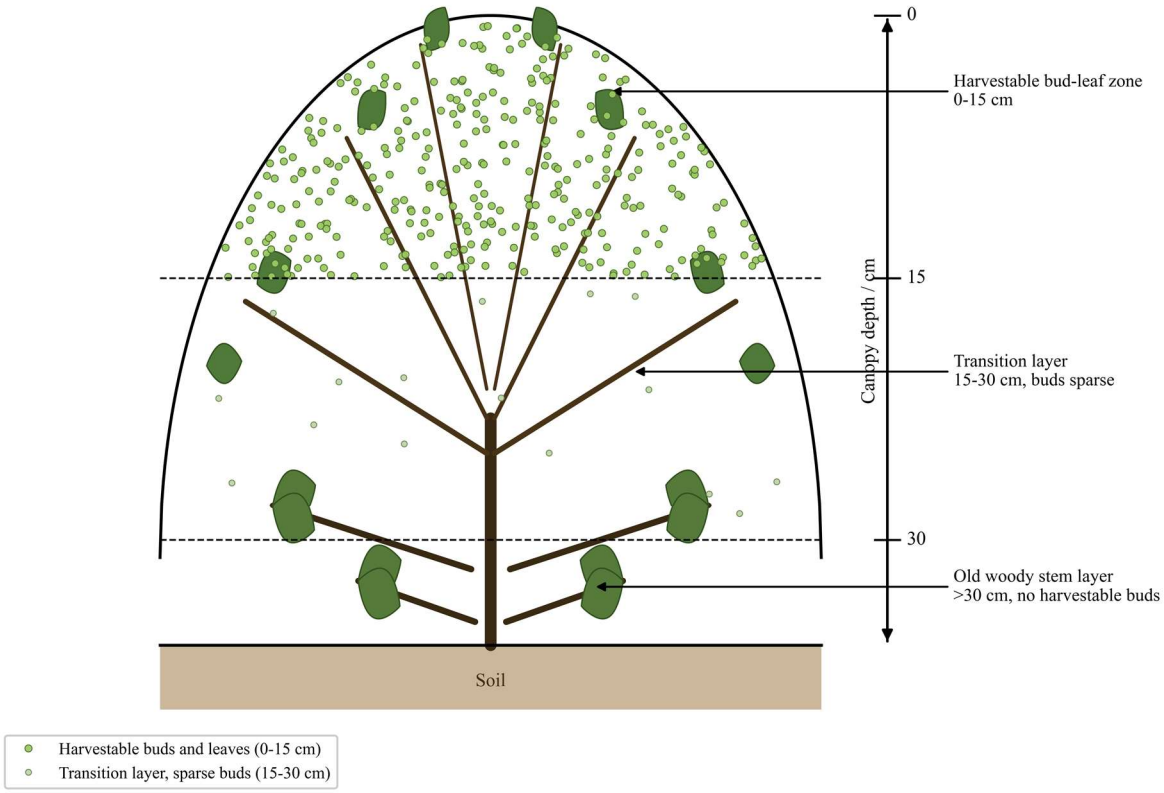


Figure 3. Schematic diagram of the spatial distribution of buds and leaves in the tea canopy.

ISSN: 2664-9640

3.2. Modelling the Spatial Distribution of the Harvesting Targets

To describe the spatial distribution of the buds and leaves quantitatively, a statistical modelling approach is adopted here to establish a spatial distribution model of the harvesting target points. It is assumed that, within the depth d below the canopy surface, the horizontal distribution of the buds and leaves follows a two-dimensional Gaussian mixture distribution while the vertical distribution follows an exponential decay law.

Let the height function of the canopy surface be $h(x, y)$; the density function of the buds and leaves at depth z can then be written as

$$\rho(x, y, z) = \rho_0 \cdot exp\left(-\frac{h(x,y)-z}{\lambda}\right) \cdot \sum_{k=1}^{K} w_k \cdot \mathcal{N}((x, y); \boldsymbol{\mu}_k, \Sigma_k) \tag{14}$$

where ρ_0 is the reference density at the canopy surface, λ is the vertical decay coefficient, K is the number of clustered regions, w_k is the weight of the k-th cluster; $\boldsymbol{\mu}_k$ and Σ_k are the mean and the covariance matrix of the k-th two-dimensional Gaussian distribution, respectively.

This model reflects the non-uniformity and the clustering of the bud and leaf distribution and provides a theoretical basis for the region partitioning used in the subsequent path planning. In practice, the model parameters can be obtained by fitting after the canopy has been scanned by a vision system to acquire point-cloud data.

3.3. Matching between the Harvesting Space and the Manipulator Workspace

The workspace of the Delta manipulator is approximately dome-shaped, being wide in the upper part and tapering towards the bottom, whereas the tea canopy usually presents an arched plucking table, so the two spatial forms differ. To evaluate the ability of the manipulator to cover the harvesting space, the matching between the workspace and the harvesting space must be quantified. For the structural parameters adopted in Section 5.1, the workspace determined as described in Section 2.4.1 has a maximum horizontal diameter of 340 mm, a vertical extent of 219 mm and a volume of 5250 cm^3, the widest section lying 200 mm below the fixed platform.

Let the harvesting region be the space within the depth D below the canopy surface, denoted by $\mathcal{S}_p$, and let the workspace of the manipulator be denoted by $\mathcal{W}$. The coverage ratio of the harvesting space by the workspace is then defined as

$$\eta = \frac{V(\mathcal{S}_p \cap \mathcal{W})}{V(\mathcal{S}_p)} \tag{15}$$

where $V(\cdot)$ denotes spatial volume.

The coverage ratio η reflects the degree of accessibility of the harvesting region by the manipulator. The higher the coverage ratio, the larger the proportion of harvesting target points that the manipulator can reach. The factors influencing the coverage ratio include the structural parameters of the manipulator, the installation height, and the size and shape of the harvesting region. Because the workspace tapers downwards, the installation height has a strong influence on the coverage ratio: for an arched canopy 800 mm wide with an arch rise of 100 mm and a harvesting depth of 50 mm, the coverage ratio falls from 3.1 % when the crown of the canopy surface lies 200 mm below the fixed platform to 1.7 % at 223 mm and 0.4 % at 250 mm. Placing the canopy surface as close as possible to the widest section of the workspace is therefore essential.

For a single Delta manipulator with the parameters of Section 5.1 the workspace diameter reaches at most 340 mm, which is far from sufficient to cover the harvesting region of an entire

ISSN: 2664-9640

row of tea plants at one time. In practice the operating range can be enlarged by arranging an array of manipulators or by carrying the manipulator on a mobile platform. In either case the manipulator repeatedly traverses a single workspace-sized sub-region, so the efficiency of the harvesting operation is governed by how well the path within one workspace is planned. This paper therefore focuses on the harvesting path planning of a single Delta manipulator within the coverage of its workspace.

4. Path Planning of the Delta Manipulator for Premium-tea Harvesting

4.1. Problem Statement and Evaluation Indices

The path-planning problem of premium-tea harvesting can be stated as follows: within the workspace of the manipulator, given the spatial coordinates of N buds and leaves to be harvested, plan a motion path that starts from the initial point, traverses all harvesting points and returns to the initial point, such that the total harvesting time is minimised or the overall performance is optimal while the kinematic constraints of the Delta manipulator (joint angle limits, velocity constraints, acceleration constraints and avoidance of singular configurations) are satisfied.

This problem is essentially a constrained travelling salesman problem (TSP). Unlike the conventional TSP, the premium-tea harvesting scenario involves a large number of target points that are densely and in part clustered in space, and the path must satisfy the kinematic constraints of the manipulator, so the straight-line distance cannot simply be used as the cost function.

The following evaluation indices are selected in this paper to measure the performance of path planning.

Harvesting efficiency, that is the number of plucking operations completed per unit time, is the core index of the operational capability of a harvesting robot. In path planning, the shorter the total harvesting time, the higher the efficiency.

Trajectory smoothness reflects the variation of velocity and acceleration during the motion of the manipulator. Jerk is a commonly used measure of trajectory smoothness: the smaller the jerk, the smoother the motion and the smaller the impact on the mechanical structure [11].

Path length is the total length of the trajectory of the end effector. It directly affects the motion time and the energy consumption.

Singularity avoidance indicates whether the path passes through or close to a region of singular configurations. It can be assessed by the maximum and the average value of the condition number of the Jacobian matrix along the path.

4.2. Conventional Methods and Their Limitations

Conventional multi-target path-planning methods mainly comprise intelligent optimisation algorithms such as the genetic algorithm, the ant colony algorithm and simulated annealing. These algorithms perform well on small-scale TSP instances, but in the premium-tea harvesting scenario they face the following problems.

Large number of target points. Between tens and hundreds of harvesting points may be distributed within the workspace of a single Delta manipulator. As the number of target points increases, the solution space of the TSP grows exponentially and the computational efficiency of conventional algorithms falls sharply.

Non-uniform spatial distribution. The buds and leaves are distributed in clusters within the canopy, with dense and sparse regions alternating. Conventional algorithms search uniformly over the whole domain, fail to exploit the clustering of the distribution and readily generate redundant paths in locally dense regions.

ISSN: 2664-9640

Difficulty in handling kinematic constraints. The conventional TSP usually takes the Euclidean distance as the cost function, whereas the actual motion time of a Delta manipulator depends not only on distance but also on joint velocity constraints, acceleration constraints and singular configurations. Approximating the cost directly by the straight-line distance leads to a substantial deviation between the planned result and the actual motion.

4.3. Hierarchical Path Planning based on Density Clustering

To address the above problems, a hierarchical path-planning method based on density clustering is proposed. Its central idea is to exploit the clustering of the spatial distribution of the buds and leaves in order to decompose the global planning problem into two levels, namely macro path planning between clusters and micro path planning within clusters, thereby reducing the problem size and improving the solution efficiency.

4.3.1. Clustering of the Harvesting Points by DBSCAN

The density-based spatial clustering of applications with noise (DBSCAN) algorithm is used to cluster the harvesting target points. DBSCAN does not require the number of clusters to be specified in advance, can discover clusters of arbitrary shape and can identify noise points, and is therefore well suited to the non-uniform distribution of buds and leaves.

The core concepts of DBSCAN are the neighbourhood radius ε and the minimum number of samples $MinPts$. Let the data set of harvesting points be D and an arbitrary harvesting point be p. The spatial separation between points is measured by the Euclidean distance. The core formulae are as follows.

(1) Definition of the neighbourhood of a harvesting point

$$N_{\varepsilon}(p) = \{q \in D \mid d(p,q) \leq \varepsilon\} \tag{16}$$

Here $N_{\varepsilon}(p)$ is the set of neighbouring harvesting points of the point p, ε is the prescribed neighbourhood radius, corresponding to the effective spatial neighbourhood of a bud or leaf during harvesting, and $d(p,q)$ is the Euclidean distance between two points, which measures the spatial spacing of the buds and leaves.

(2) Criterion for a core harvesting point

$$|N_{\varepsilon}(p)| \geq MinPts \tag{17}$$

A harvesting point p satisfying the above expression is judged to be a core point, which indicates that the buds and leaves are densely distributed in that region and can form an effective harvesting cluster. All harvesting points that are density-reachable or density-connected from core points together constitute a complete harvesting cluster, whereas sparse and isolated abnormal bud and leaf points are identified as noise and removed.

In the premium-tea harvesting scenario, the choice of the clustering parameters is related to the density of the bud and leaf distribution and to the motion characteristics of the manipulator. The neighbourhood radius can be set according to the mean spacing of the buds and leaves, while $MinPts$ reflects the minimum size of an effective harvesting cluster.

After clustering, each cluster is regarded as a sub-region for harvesting. For each cluster its centre is computed as the representative point of the sub-region. Let a cluster contain k harvesting points with coordinates (x_i, y_i); the geometric centre of the cluster is given by

$$(X_c, Y_c) = \left(\frac{1}{k}\sum_{i=1}^{k} x_i, \frac{1}{k}\sum_{i=1}^{k} y_i\right) \tag{18}$$

ISSN: 2664-9640

where (X_c, Y_c) is the centre of the sub-region cluster, which represents the spatial position of the whole cluster and provides the node basis for macro path planning.

4.3.2. Macro Path Planning between Clusters

Macro path planning between clusters determines the traversal order of the sub-regions. Since the number of clusters is much smaller than the number of original target points, the size of the problem at this level is greatly reduced.

The centre of each cluster is treated as a city node of the TSP, and an improved ant colony algorithm is used to solve for the optimal traversal order between clusters. The ant colony algorithm seeks the optimal path by simulating the pheromone mechanism of ants foraging, and is characterised by positive feedback, distributed computation and strong robustness [12].

The macro path planning between clusters is essentially a TSP optimisation with the cluster centres as nodes and the shortest global harvesting path as the optimisation objective. Rather than repeating the standard ant colony transition formula, a path-cost objective function together with an elitist iterative update strategy is adopted to obtain the optimal traversal sequence. The core mathematical model is as follows.

Let the total number of clustered sub-regions be n, let the spatial distance between any two cluster centres i, j be d_{ij}, and define a 0-1 decision variable x_{ij} such that i if the path goes from cluster j to cluster $x_{ij=1}$ and $x_{ij} = 0$ otherwise. The objective function of the macro path optimisation between clusters is

$$\min \quad F = \sum_{i=1}^{n} \sum_{j=1}^{n} d_{ij} x_{ij} \tag{19}$$

Here F is the total length of the global harvesting path between clusters; minimising it yields the optimal traversal order of the sub-regions. In accordance with the constraints of the premium-tea harvesting scenario, each cluster must be visited exactly once and the path must be a closed loop without repeated traversal, that is $\sum_{i=1}^{n} x_{ij} = 1$ and $\sum_{j=1}^{n} x_{ij} = 1$.

To improve the accuracy of the macro path solution, the elitist retention strategy of the improved ant colony algorithm is adopted, in which the pheromone update is reinforced separately for the best path of the iteration, according to

$$\tau_{ij}(t+1) = (1-\rho)\tau_{ij}(t) + \Delta\tau_{ij}^{best}(t) \tag{20}$$

where $\Delta\tau_{ij}^{best}(t) = Q/F_{best}$ and F_{best} is the length of the best cluster traversal path of the current iteration. This strategy releases pheromone only on the best path, reinforcing the positive feedback in favour of high-quality paths, improving the convergence speed and the solution accuracy of the macro path, and meeting the engineering requirement of batch traversal of harvesting regions.

4.3.3. Micro Path Planning within Clusters

Once the cluster traversal order has been determined, micro path planning is carried out for the harvesting points inside each cluster. The number of target points within a cluster is relatively small and their spatial distribution is concentrated, so an exact algorithm or an improved heuristic algorithm can be used.

For small clusters (for example fewer than ten points) the optimal path can be solved exactly by dynamic programming. For larger clusters the ant colony algorithm is used again.

In the micro path planning within a cluster, the entry and exit points must be taken into account, that is the exit point of the preceding cluster serves as the entry point of the current cluster and

ISSN: 2664-9640

the exit point of the current cluster serves as the entry point of the next cluster. This guarantees the continuity of the path between clusters and avoids additional detours.

Let the optimal exit point of the preceding cluster have coordinates $S_{in}(x_0, y_0)$, and let the set of all harvesting points of the current cluster be $V = \{v_1, v_2, \ldots, v_n\}$. The objective of the micro path planning within the cluster is to minimise the total travelling distance during harvesting, with the objective function

$$\min L = \sum_{i=0}^{n-1} d\,(v_i, v_{i+1}) \tag{21}$$

where $v_0 = S_{in}$ is the entry point of the cluster, $d(v_i, v_{i+1})$ is the travelling distance between adjacent harvesting points, and L is the total harvesting path length within the cluster. Minimising the total path length yields the optimal harvesting path within a single cluster. At the same time the optimal exit point of the current cluster is defined as S_{out} and serves as the entry constraint of the cluster at the next level, so that a continuous hierarchical harvesting path without redundancy is formed over the whole route.

4.3.4. Principle of the Ant Colony Optimisation (ACO) Algorithm

In 1992, Marco Dorigo proposed the ant colony optimisation (ACO) algorithm for the first time in his doctoral thesis, based on the foraging behaviour of real ants. While searching for a food source, an ant deposits a pheromone on the path it has travelled and is able to perceive the pheromone deposited by other ants. The concentration of the pheromone represents the length of the path: the higher the concentration, the shorter the corresponding path.

As a rule, ants preferentially choose paths of higher pheromone concentration with a larger probability and deposit a certain amount of pheromone, thereby increasing the pheromone concentration on that path and forming a positive feedback. Eventually the ants find the best path from the nest to the food source, that is the shortest path. The pheromone concentration on the paths decays gradually as time progresses [13].

n: number of nodes;

m: number of ants;

t: iteration instant; $\tau_{ij}(t)$: pheromone concentration on edge $(i \to j)$ at instant t;

η_{ij}: heuristic function, equal to the reciprocal of the distance in the TSP;

$\eta_{ij} = \frac{1}{d_{ij}}$; (d_{ij}): Euclidean distance from node i to node j;

$allowed_k$: set of nodes not yet visited by ant k;

α: importance factor of the pheromone; β: importance factor of the heuristic;

ρ: pheromone evaporation coefficient, $0 < \rho < 1$;

Q: constant of pheromone release intensity;

L_k: total length of the path of ant k in the current round.

At the initial instant of the algorithm, the m ants are placed randomly on the n cities and the first element of the tabu list of each ant is set to the city in which it is currently located. At this moment the amount of pheromone on every path is equal, the initial pheromone on every edge being a small constant $\tau_{ij}(0)=c$((a small constant)). The probability that at instant t an ant moves from city i to city j is

$$p_{ij}^{k}(t) = \begin{cases} \dfrac{[\tau_{ij}(t)]^{\alpha} \cdot [\eta_{ij}]^{\beta}}{\sum_{s \in allowed_k} [\tau_{is}(t)]^{\alpha} \cdot [\eta_{is}]^{\beta}}, j \in allowed_k \\ 0, \text{otherwise} \end{cases} \tag{22}$$

ISSN: 2664-9640

where $\tau_{ij}(t)$ is the pheromone concentration on the path from cluster centre t to i at instant j, $\eta_{ij} = 1/d_{ij}$ is the heuristic factor representing the reciprocal of the cluster spacing, α, β are the weights of the pheromone and of the heuristic factor, respectively, and $allowed_k$ is the set of sub-regions not yet traversed.

After all ants have completed their path search, the pheromone on each edge is updated using the ant-cycle model:

$$\tau_{ij}(t+1) = (1-\rho)\tau_{ij}(t) + \sum_{k=1}^{m} \Delta\, \tau_{ij}^{k} \tag{23}$$

This consists of two parts.

(1) $(1-\rho)\tau_{ij}(t)$: pheromone evaporation. ρ is the evaporation coefficient and the old pheromone decays proportionally, which prevents the algorithm from converging prematurely to a local optimum. The larger ρ, the more intense the evaporation.

(2) $\sum_{k=1}^{m} \Delta\, \tau_{ij}^{k}(t)$: total pheromone increment of all ants.

Pheromone increment $\Delta\tau_{ij}^{k}(t)$ (ant-cycle global update model):

$$\Delta\tau_{ij}^{k}(t) = \begin{cases} \frac{Q}{L_k}, \text{if ant k traverses edge}(i,j) \\ 0, \text{otherwise} \end{cases} \tag{24}$$

Ant-quantity (step update):

$$\Delta\tau_{ij}^{k} = \frac{Q}{d_{ij}} \tag{25}$$

Ant-density (step update):

$$\Delta\tau_{ij}^{k} = Q \tag{26}$$

At the start of the algorithm all edges are assigned an initial pheromone:

$$\tau_{ij}(0) = \tau_0 \tag{27}$$

τ_0 is a constant, generally a small fixed value; the improved MMAS algorithm sets lower and upper bounds $\tau_{\min}, \tau_{\max}$ on the pheromone. Conventional ACO-based Optimal Path Plot and Iterative Convergence Curve Plot is shown in Figure 4.

ISSN: 2664-9640

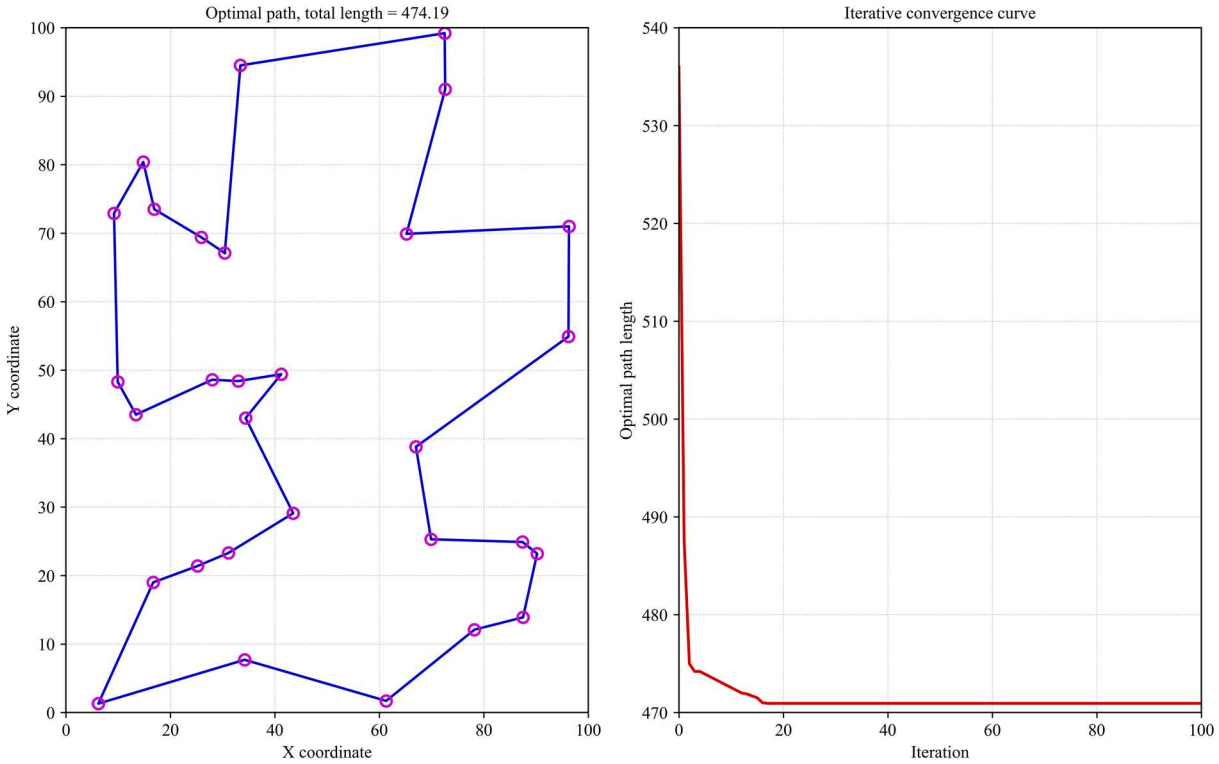


Figure 4. Conventional ACO: (a) optimal path; (b) iterative convergence curve.

4.3.5. Improved Ant Colony Algorithm (DBSCAN-ACO)

In view of the uneven spatial distribution of premium-tea buds and leaves and the strong blindness, slow convergence and susceptibility to local optima of the conventional ant colony path planning, this paper combines the advantages of density clustering and of the ant colony algorithm to construct a DBSCAN-ACO hybrid path-optimisation algorithm. The algorithm follows the solution strategy of "clustering and partitioning first, hierarchical optimisation afterwards": DBSCAN is used to perform adaptive clustering and noise filtering of the harvesting points, which reduces the solution dimension; the ant colony algorithm is then improved on the basis of the cluster density characteristics to obtain the hierarchical optimum of the macro path between clusters and the micro path within clusters. This effectively improves the efficiency and the accuracy of harvesting path planning in complex field scenarios.

The DBSCAN algorithm is used to carry out density clustering preprocessing of the discrete harvesting points, adaptively partitioning the harvesting sub-regions and removing discrete invalid noise points, so as to provide a structured data basis for the dimensionality reduction of the subsequent ant colony optimisation. The core mathematical definitions are as follows.

Definition of the neighbourhood of a harvesting point:

$$N_\varepsilon(p) = \{q \in D \mid d(p,q) \le \varepsilon\} \tag{28}$$

Here D is the data set of harvesting points, ε is the prescribed neighbourhood radius and $N_\varepsilon(p)$ is the set of neighbouring points of the harvesting point p.

Criterion for the density of a core point:

$$|N_\varepsilon(p)| \ge MinPts \tag{29}$$

ISSN: 2664-9640

A harvesting point satisfying the above expression is a core point; the point set formed by points that are density-connected from core points constitutes an effective harvesting cluster, while discrete points that do not satisfy the density condition are judged to be noise and removed. In order to reduce the dimensionality of the macro path, the geometric centre of each cluster is computed as the representative node of the sub-region:

$$(X_c, Y_c) = \left(\frac{1}{k}\sum_{i=1}^{k} x_i, \frac{1}{k}\sum_{i=1}^{k} y_i\right) \tag{30}$$

Here k is the number of harvesting points in a single cluster, (x_i, y_i) are the coordinates of the harvesting points and (X_c, Y_c) are the coordinates of the cluster centre.

The conventional ant colony algorithm searches for a path on the basis of distance information alone and does not consider the density distribution of the buds and leaves. In this paper the heuristic function and the pheromone update rule are reconstructed in combination with the DBSCAN clustering result, so as to build an improved ant colony algorithm suitable for hierarchical harvesting path planning.

(1) Density-adaptive heuristic function

A correction factor based on the areal density of the cluster is introduced so that the algorithm traverses high-density harvesting regions preferentially, which accords with the actual practice of harvesting. The expression is

$$\eta_{ij} = \frac{\rho_i}{d_{ij}}, \quad \rho_i = \frac{|N_\varepsilon(p_i)|}{S_i} \tag{31}$$

Here η_{ij} is the improved heuristic factor, ρ_i is the areal density of the i-th cluster, $|N_\varepsilon(p_i)|$ is the number of effective harvesting points in the cluster, S_i is the area covered by the cluster and d_{ij} is the spacing between cluster centres.

(2) Hierarchical state transition probability

Taking the clustering partition constraint into account, an ant selects the next node to traverse on the basis of the pheromone concentration and the density heuristic information. The transition probability is

$$p_{ij}^{k}(t) = \begin{cases} \dfrac{[\tau_{ij}(t)]^{\alpha}\cdot[\eta_{ij}]^{\beta}}{\sum_{s\in allowed_k}[\tau_{is}(t)]^{\alpha}\cdot[\eta_{is}]^{\beta}}, j \in allowed_k \\ 0, \text{otherwise} \end{cases} \tag{32}$$

Here α and β are the pheromone weight and the heuristic factor weight, respectively, and $allowed_k$ is the set of nodes not yet traversed.

The expression is simultaneously applicable to the two-level path planning: at the macro level the cluster centres are the search nodes and the overall cluster density determines the region traversal order; at the micro level the harvesting points within a cluster are the search nodes and the local density governs the fine path optimisation. By changing the search node set and the density value, the model achieves “one formula, two-level adaptive optimisation”, which greatly simplifies the mathematical model while preserving the innovative mechanism of the algorithm.

(3) Hierarchically differentiated pheromone update

ISSN: 2664-9640

To adapt to the macro and micro two-level planning scenario, weight coefficients are introduced to differentiate the update priority of the two levels, and a hierarchical pheromone update formula is constructed:

$$\tau_{ij}(t+1) = (1-\rho)\tau_{ij}(t) + \omega_1 \Delta\tau_{ij}^{macro} + \omega_2 \Delta\tau_{ij}^{micro} \tag{33}$$

$$\Delta\tau_{ij} = \frac{Q}{L_{best}} \tag{34}$$

Here ρ is the pheromone evaporation coefficient, $\omega_1 + \omega_2 = 1$ are the weights of the macro and micro paths, respectively, Q is the pheromone intensity and L_{best} is the length of the hierarchical optimal path; the pheromone is reinforced only on the optimal path, which improves the convergence speed.

The overall procedure of the hybrid algorithm is as follows. First, the parameters are initialised and the harvesting points are partitioned by DBSCAN clustering, noise points are removed and the cluster centres are computed. Second, with the cluster centres as nodes, the improved ant colony algorithm is used to solve for the macro optimal traversal order between clusters. Finally, micro path planning is carried out inside each cluster and, together with the entry and exit constraints, the globally continuous harvesting path is assembled. DBSCAN-ACO Fusion Optimal Path Plot and Iterative Convergence Curve Plot is shown in Figure 5.

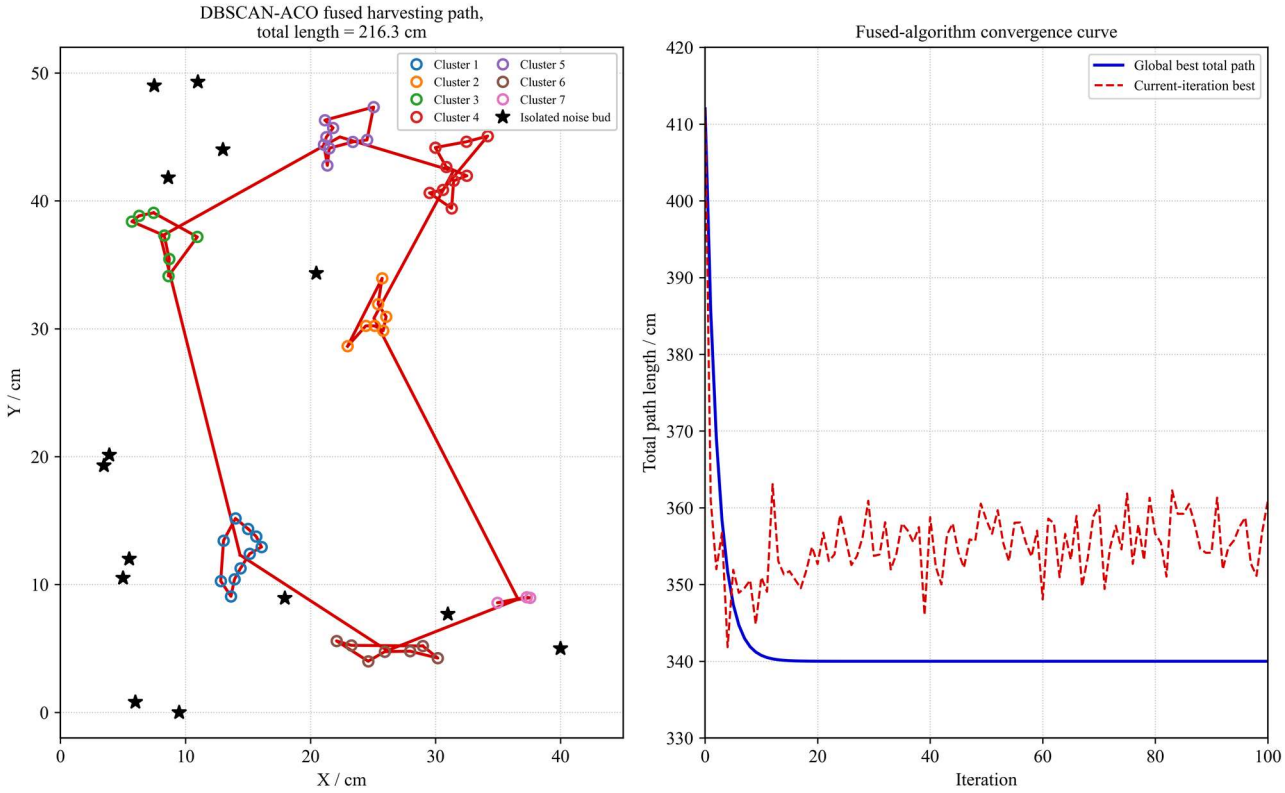


Figure 5. DBSCAN-ACO fusion: (a) optimal path with the detected clusters; (b) iterative convergence curve.

By means of clustering preprocessing the hybrid algorithm reduces the dimensionality of the search and overcomes the blindness of the conventional ant colony algorithm; the density-adaptive improvement incorporates the characteristics of the bud and leaf distribution,

ISSN: 2664-9640

effectively avoiding premature convergence and giving the algorithm greater adaptability and solution stability in scenarios with an uneven distribution of buds and leaves.

4.4. Trajectory Smoothing Subject to Kinematic Constraints

The path obtained by hierarchical planning is a polyline consisting of a series of discrete harvesting points. At the corners of such a polyline the direction of the velocity changes abruptly, which causes a sharp increase in the joint acceleration and jerk, and thus affects the smoothness of the motion and the service life of the mechanism. The path must therefore be smoothed.

In this paper a quintic B-spline curve is used to interpolate the path smoothly. B-spline curves offer local support, the convex-hull property and geometric invariance, and can realise smooth trajectories of high-order continuity [14].

Let the path contain n harvesting points $Q_0, Q_1, \dots, Q_{n-1}$. A quintic B-spline curve is constructed in Cartesian space so that it passes through all the harvesting points in turn. The basis functions of the quintic B-spline are defined by the de Boor recursion formula and the curve is expressed as

$$\boldsymbol{P}(u) = \sum_{i=0}^{n-1} N_{i,5}(u) \cdot \boldsymbol{d}_i \tag{35}$$

where $\boldsymbol{d}_i$ are the control vertices and $N_{i,5}(u)$ are the quintic B-spline basis functions.

By back-computing the control vertices, the B-spline curve is made to interpolate all the harvesting points. A quintic B-spline curve guarantees the continuity of position, velocity, acceleration and even jerk, and effectively reduces the impact and vibration during motion.

In trajectory planning the kinematic constraints of the Delta manipulator must also be taken into account. The trajectory in Cartesian space is mapped to joint space by the inverse position solution, and the angle, angular velocity and angular acceleration of each joint are checked against the permissible ranges. If a constraint is violated, the time distribution of the trajectory must be adjusted or the path must be replanned. Flowchart of the hierarchical path-planning method is shown in Figure 6.

To avoid singular configurations, a singularity penalty term is introduced in the path planning. When the condition number of the Jacobian matrix at a point of the path exceeds a threshold, a corresponding penalty is added to the cost function so as to guide the path away from the singular region [15].

ISSN: 2664-9640

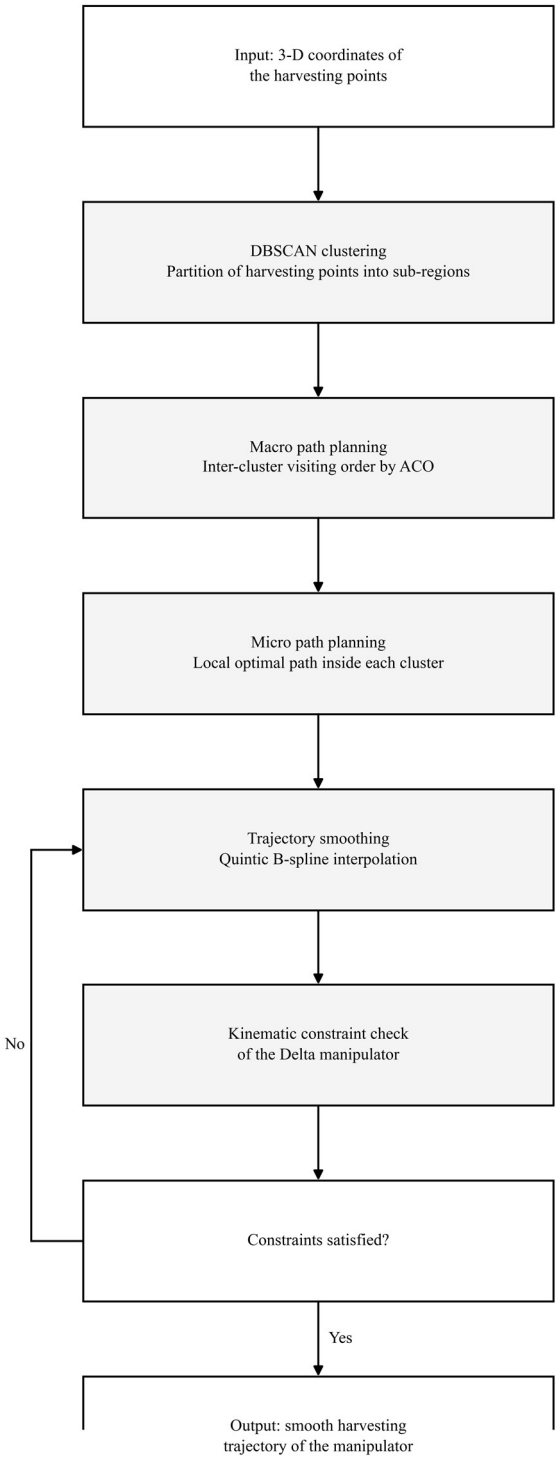


Figure 6. Flowchart of the hierarchical path-planning method.

5. Simulation Experiments and Discussion

5.1. Simulation Environment and Parameter Settings

To verify the effectiveness of the proposed method, a simulation platform was built in the MATLAB environment. The structural parameters of the Delta manipulator were set with reference to a typical harvesting application: the radius of the fixed platform is $R = 150$ mm, the radius of the moving platform is $r = 50$ mm, the length of the drive arm is $L = 200$ mm and the length of the driven arm is $l = 400$ mm. The range of the drive angle was set to $-90^\circ \sim 30^\circ$.

ISSN: 2664-9640

The harvesting target points were generated with the spatial distribution model established in Section 3. The canopy surface was set to be arched with an arch rise of 100 mm, the canopy width was 800 mm and the bud and leaf distribution depth was 50 mm. The crown of the canopy surface was placed 200 mm below the fixed platform, which, as shown in Section 3.3, brings the harvesting layer as close as possible to the widest section of the workspace. Sixty harvesting target points were generated within the workspace in order to simulate the distribution of buds and leaves in the premium-tea harvesting scenario.

The methods compared were the conventional ant colony algorithm (ACO) solving the global TSP directly, the genetic algorithm (GA) solving the global TSP, and the hierarchical path-planning method based on DBSCAN clustering (DBSCAN-ACO) proposed in this paper.

5.2. Kinematic Verification

The kinematic model of the Delta manipulator was verified first. Several typical pose points were selected and the inverse and forward position solutions were computed by the analytical method and by the numerical method; the results were compared in order to verify the correctness of the model. Inverse position solution verification results is shown in Table 1.

Table 1. Inverse position solution verification results

End-effector position (mm)	Drive angle θ1 (°)	Drive angle θ2 (°)	Drive angle θ3 (°)	Error (mm)
(0, 0, −350)	−23.6	−23.6	−23.6	0.001
(50, 50, −380)	−18.2	−31.5	−28.7	0.003
(100, 0, −360)	−10.5	−32.1	−32.1	0.002
(80, −60, −400)	−15.8	−28.3	−38.9	0.004

The verification results show that the computational accuracy of the kinematic model meets the requirements, the error of the inverse solution being of the order of micrometres, so that the model can be used for the subsequent path planning and trajectory generation.

5.3. Comparative Path-planning Experiments

With the same sixty harvesting target points, path planning was carried out by the three methods and the results are compared in Table 2.

Table 2. Comparison of the different path-planning methods

Evaluation index	Conventional ACO	Conventional GA	DBSCAN-ACO	Improvement
Total path length (mm)	2856.3	2943.7	2432.5	14.8 %
Total harvesting time (s)	12.8	13.5	10.4	18.8 %
Maximum jerk (mm/s^3)	3.87×10^5	4.21×10^5	2.55×10^5	34.1 %
Average condition number	4.62	4.85	3.98	13.9 %
Computation time (s)	45.2	68.7	12.6	72.1 %

It can be seen from Table 2 that the proposed hierarchical DBSCAN-ACO path-planning method outperforms the conventional global optimisation methods in every index. The total path length is reduced by 14.8 %, the total harvesting time by 18.8 % and the computation time by 72.1 %. This is mainly because the hierarchical strategy effectively reduces the size of the problem and exploits the clustering characteristics to eliminate redundant paths.

With regard to trajectory smoothness, after smoothing and optimisation with the quintic B-spline the maximum jerk is reduced by 34.1 %, so that the smoothness of the motion is significantly improved. The average condition number is also reduced, which indicates that the path avoids part of the high-condition-number region and that the singularity avoidance performance is good.

ISSN: 2664-9640

5.4. Tests under Different Distribution Scenarios

To verify the adaptability of the method under different distribution scenarios, three typical distributions were tested: uniform, random and clustered. Sixty harvesting target points were generated in each scenario and the experiment was repeated ten times, the average being taken. The results obtained are shown in Table 3.

Table 3. Performance comparison under different distribution scenarios

Distribution scenario	Method	Path length (mm)	Harvesting time (s)	Computation time (s)
Uniform	Conventional ACO	2715.6	12.1	43.8
Uniform	DBSCAN-ACO	2543.2	11.0	15.3
Random	Conventional ACO	2856.3	12.8	45.2
Random	DBSCAN-ACO	2432.5	10.4	12.6
Clustered	Conventional ACO	3124.8	14.2	48.6
Clustered	DBSCAN-ACO	2387.6	9.8	8.7

The test results show that the advantage of the proposed method is most pronounced in the clustered distribution scenario, where the path length is shortened by 23.6 % and the harvesting time is reduced by 31.0 %. This is because the clustering of the buds and leaves is more pronounced in this scenario and the hierarchical strategy can exploit this characteristic more fully in order to eliminate redundant paths. In the uniform distribution scenario the clustering is less evident and the improvement achieved by the method is correspondingly smaller.

6. Conclusion

Aiming at the requirements of fine premium-tea harvesting, this paper has studied the kinematic analysis and the harvesting path planning of a Delta parallel manipulator. A kinematic model of the Delta manipulator was established, the forward and inverse position solutions and the velocity Jacobian matrix were derived, and the workspace and singular configurations were analysed. On the basis of the distribution of buds and leaves in the tea canopy, a spatial distribution model of the harvesting target points was established and the matching between the manipulator workspace and the harvesting space was evaluated. A hierarchical path-planning method based on DBSCAN density clustering was proposed, which decomposes the global planning into macro planning between clusters and micro planning within clusters and uses a quintic B-spline curve for trajectory smoothing while taking the kinematic constraints and singularity avoidance into account.

The simulation results show that, compared with the conventional global ant colony algorithm, the proposed method reduces the total path length by 14.8 %, the total harvesting time by 18.8 % and the maximum jerk by 34.1 %, and improves the computational efficiency by 72.1 %. The advantage is even more pronounced in the clustered distribution scenario, and the method adapts better to the unstructured environment of premium-tea harvesting. The effectiveness of the method provides a theoretical basis and a technical reference for the application of the Delta manipulator to premium-tea harvesting.

Some limitations of this study remain. The present work is based mainly on simulation and physical prototype experiments have not yet been carried out; the spatial distribution model adopts a statistical modelling approach and may deviate from the actual distribution of buds and leaves in a real tea canopy; and the time consumed by the plucking action itself and the

ISSN: 2664-9640

orientation adjustment of the end effector are not considered in the path planning. The coverage analysis of Section 3.3 also shows that a single manipulator with these structural parameters reaches only about 3 % of the harvesting region of an 800 mm canopy, so that an array of manipulators or a mobile platform is indispensable in practice; the cooperative planning of several manipulators has not been addressed here. Future work will therefore address the development of a physical prototype, the acquisition of real canopy data and the corresponding modelling, complete path planning that takes the plucking action into account, and the coordinated planning of multiple manipulators.

References

[1] Yang, H. L., Zhong, Y., Jiang, Y. Z., et al. (2022). Hybrid strategy of trajectory planning for a parallel tea-plucking robot based on optimal time and jerk. Journal of Mechanical Engineering, 58(18), 212–221. (in Chinese)

[2] Wu, L., Liu, H., Ye, C., et al. (2024). Development of a premium tea-plucking robot integrating deep learning and machine vision. Applied Sciences, 14(13), 5748.

[3] Zhong, Y., Deng, F., & Li, M. (2021). Computer vision-based high-quality tea automatic plucking robot using Delta parallel manipulator. Computers and Electronics in Agriculture, 181, 105946.

[4] Gosselin, C., & Angeles, J. (1990). Singularity analysis of closed-loop kinematic chains. IEEE Transactions on Robotics and Automation, 6(3), 281–290.

[5] Zlatanov, D., Bonev, I. A., & Gosselin, C. M. (2002). Constraint singularities of parallel mechanisms. In Proceedings of the 2002 IEEE International Conference on Robotics and Automation (pp. 496–501). IEEE.

[6] Jia, J. M., Wang, D. Y., He, L. Y., et al. (2025). Research progress and prospects of the mechanical technology of premium tea-plucking robots. Transactions of the Chinese Society for Agricultural Machinery, 56(4), 1–18. (in Chinese)

[7] Huang, Z., Zhao, Y. S., & Zhao, T. S. (1997). Theory and control of parallel robot mechanisms. China Machine Press. (in Chinese)

[8] Chen, J. N., Yu, T. J., Jia, J. M., et al. (2026). Three-dimensional path planning method for tea bud plucking based on deep reinforcement learning. Transactions of the Chinese Society for Agricultural Machinery, 57(1), 68–78. (in Chinese)

[9] Dorigo, M., Maniezzo, V., & Colorni, A. (1996). Ant system: optimization by a colony of cooperating agents. IEEE Transactions on Systems, Man, and Cybernetics, Part B (Cybernetics), 26(1), 29–41.

[10] Ester, M., Kriegel, H.-P., Sander, J., et al. (1996). A density-based algorithm for discovering clusters in large spatial databases with noise. In Proceedings of the 2nd International Conference on Knowledge Discovery and Data Mining (pp. 226–231). AAAI Press.

[11] Zhu, X. Q., Zhang, F., & Qin, Y. Q. (2020). High-order continuous trajectory planning of a Delta robot using quintic B-splines. Machine Design and Manufacturing Engineering, 49(6), 71–75. (in Chinese)

[12] Li, X., & Wang, J. (2018). Design of a four-DOF gantry tea-picking robot based on a DSP controller. Journal of Agricultural Machinery, 49(S1), 123–129.

[13] Wang, H., & Guan, Y. (2020). Trajectory tracking of a SCARA tea-picking manipulator using neural network adaptive compensation control. Transactions of the Chinese Society for Agricultural Machinery, 51(7), 34–41.

[14] Abhiram, S., & Kumar, A. (2021). Review on development of tea harvesting machines. Agricultural Reviews, 42(2), 137–145.

[15] Laribi, M. A., Romdhane, L., & Zeghloul, S. (2007). Analysis and dimensional synthesis of the DELTA robot for a prescribed workspace. Mechanism and Machine Theory, 42(7), 859–870.